AIP | Applied Physics Letters

Confined energy states in quantum dots detected by a resonant differential capacitance method

O. Engström, M. Kaniewska, and M. Kaczmarczyk

Citation: Applied Physics Letters **95**, 013104 (2009); doi: 10.1063/1.3168408
View online: http://dx.doi.org/10.1063/1.3168408
View Table of Contents: http://scitation.aip.org/content/aip/journal/apl/95/1?ver=pdfcov
Published by the AIP Publishing

Confined energy states in quantum dots detected by a resonant differential capacitance method

O. Engström,[1] M. Kaniewska,[2,a)] and M. Kaczmarczyk[2]
[1]*Chalmers University of Technology, Microtechnology and Nanoscience, SE-412 96 Göteborg, Sweden*
[2]*Department of Analysis of Semiconductor Nanostructures, Institute of Electron Technology, Al. Lotnikow 32/46, Warsaw 02-668, Poland*

(Received 6 May 2009; accepted 11 June 2009; published online 6 July 2009)

A novel method is demonstrated for revealing the presence of confined energy states in quantum dots. The samples used are Schottky diodes with quantum dots inserted in a plane inside its depletion region. By measuring the voltage derivative of the differential diode capacitance and plotting the data as contour diagrams on a voltage versus temperature plane, the confined charge carrier states are visualized as peaks. To confirm this interpretation, experimental data are compared with theory based on statistics earlier used for understanding data from deep level transient spectroscopy on the same type of samples. © *2009 American Institute of Physics*.
[DOI: 10.1063/1.3168408]

The experimental progress in understanding charge carrier interaction with quantum dots (QDs) includes two main methodologies. For the internal qualities, observed as radiative recombination of excitons, extended luminescence results have been presented in the literature for a long period of time.[1–3] Another important property of QDs for technical applications is the interaction between captured charge carriers and energy band states of the matrix material embedding these structures. Here, capacitance versus voltage (*C-V*) (Refs. 4 and 5) and deep level transient spectroscopy (DLTS) have dominated published results.[6–11] *C-V* data revealing the existence of *s* like ground states and *p* like excited states in InAs/GaAs QDs have been demonstrated by the occurrence of a detailed ripple in conveniently measured capacitance data. These early and important investigations of QDs often include sample structures prepared to magnify the influence of the excited states while otherwise hard to detect.[4]

In our present work, we have designed an extension of the *C-V* method for sample structures where InAs/GaAs QDs are embedded in a GaAs matrix and placed in the depletion region of a Schottky diode. We study the negative derivative of the capacitance as a function of applied reverse voltage and temperature of the sample. Using a three-dimensional (3D) plot with $-dC/dV$ data given on a voltage versus temperature (*V-T*) plane, electron energy states appear as peaks demonstrating the existence of exchange energies as a result of multiple carriers captured into the same type of orbital.

The QD samples were prepared by MBE in a solid source system on (001)-oriented GaAs substrates. After the deposition of a 1 μm thick buffer layer of *n*-doped (1×10^{16} cm^{-3}) GaAs at 580 °C, a 3 monolayer (ML) thick InAs film was grown at 510 °C under a repeated sequence of 0.1 ML InAs followed by a 2 *s* interruption under a continuous flux of As_2. The Stranski–Krastanov effect was observed when the thickness of the InAs film reached 2 MLs and the two-dimensional (2D) to 3D transition was saturated when the thickness reached its final value giving rise to about 10^{10} QD/cm^2. The quantum dot structures obtained where found to have base/height dimensions of about 20/10 nm. Finally a 0.4 μm thick capping layer of low doped *n*-GaAs (1×10^{16} cm^{-3}) was grown with a rate of 0.5 μm/h at 580 °C. Ohmic contact was prepared by the evaporation of gold/nickel on the backside of the highly doped wafer. The Schottky contacts were obtained by the evaporation of gold on the capping layer through a mask giving rise to circular pads with a diameter of 1 mm. *C-V* measurements were performed with an excitation amplitude of 100 mV (rms) and a frequency of 1 MHz.

The capacitance of a reverse biased Schottky diode with a QD plane positioned in the depletion region can be treated in a similar way as the capacitance of a metal-insulator-semiconductor (MIS) structure.[12,13] This requires that the depletion region extends up to or beyond the QD plane as depicted in Fig. 1. In this situation, the capping layer does not contain free charge carriers. Therefore, it is assigned to a constant capacitance, in series with the rest of the structure, given by $C_{cap}=\varepsilon\varepsilon_o/a$, where ε is the dielectric constant of the cap layer material, ε_o is the dielectric permittivity of vacuum, and a is the thickness of the layer. Starting the measurement from a voltage high enough to raise all QD energy levels above the Fermi-level of the buffer layer bulk, a second capacitance contribution, $C_{buffer}=\varepsilon\varepsilon_o/(w-a)$, occurs, given by the depletion region in this part of the sample volume. Here w is the total depth of the depletion region. Decreasing the reverse voltage, V, until the Fermi-level ap-

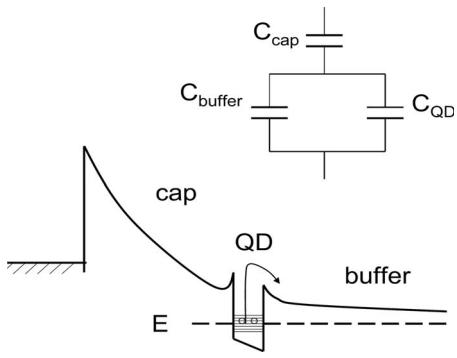

FIG. 1. Conduction band model and equivalent circuit of the Schottky diode depletion region with QDs.

a)Electronic mail: kaniew@ite.waw.pl.

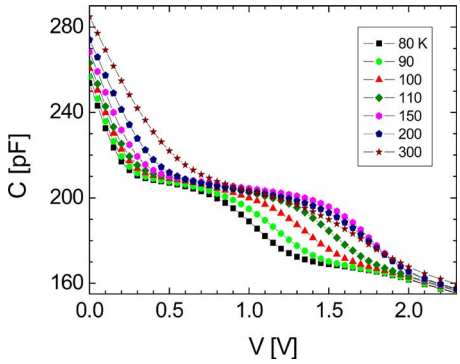

FIG. 2. (Color online) Differential capacitance as a function of reverse bias voltage at different temperatures measured with QD samples.

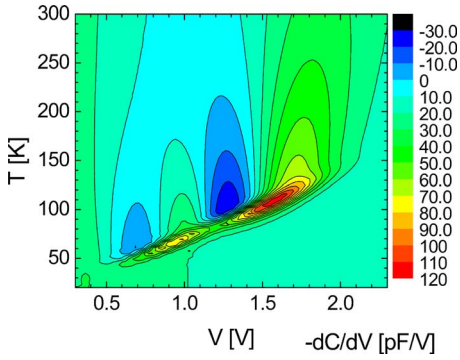

FIG. 3. (Color online) Theoretical $-dC/dV$ spectra in a contour representation on the (V,T)-plane at 1 MHz. The spectra were calculated using Eqs. (1)–(3). Two s electrons and only one p electron with average binding energy equal to 0.155 and 0.90 eV and capture cross sections of 10^{-13} and 10^{-10} cm^2, respectively, were used in the calculations. The energy distribution of QD electron states as a result of the QD size fluctuation was approximated with a Gaussian function with a standard deviation of 0.015 eV.

proaches the QD energy levels, a third contribution, C_{QD}, is added as QD electrons are captured from and thermally emitted to the conduction band of the matrix. As long as the thermal emission rate of captured electrons is larger than the angular frequency, ω, of the probe signal from the capacitance meter, C_{QD} contributes with a ledge in the total C-V graph for decreasing voltage. The total capacitance of the structure, therefore, can be described by the scheme shown in the inset of Fig. 1: a parallel connection of C_{buffer} and C_{QD} in series with C_{cap}.

Figure 2 demonstrates experimental C-V data from the structures used in the present investigation. For the graph obtained at $T=300$ K, the ledge determined by the s level occurs at about $V=2$ V with a maximum slope at about 1.8 V. As the energy levels of the QD ensemble have a certain variation due to dispersed sizes of the different dot elements,[1] the capacitance increases slightly when the voltage is lowered and the Fermi-level passes through the energy level distribution. For voltages above 2 V, the Fermi-level is below the deepest QD levels and the capacitance course is that of a common back-biased Schottky diode. In the graph shown for 100 K, the ledge has moved to a lower voltage starting at about 1.25 V. Here, the thermal emission rate of the energy levels, causing the ledge at higher voltages for the 300 K graph, has decreased to values far below the value of ω thus inhibiting electron traffic from these states. Somewhere below the 1 V level, influence from the p level would be expected when the temperature is still lowered and the capacitance ledge approaches lower voltages as the "freezing" of electron transitions continues and the Fermi-level moves higher in the QD level distribution. However, such an effect cannot be easily observed in these data. As the slopes of the ledges in Fig. 2 have a maximum when the maximum slope of the Fermi-function passes a maximum of the QD level distribution, we demonstrate below that the derivative, $-dC/dV$, resolves the level structure of s and p states.

In earlier studies of capacitance spectroscopy on QDs (Ref. 12) and in an analog case for interface states of MIS structures,[13] we have demonstrated that C_{QD} is expressed by

$$C_{\mathrm{QD}} = qA \int_{-\infty}^{\infty} \Delta n_T(\omega, e_n) \frac{df(E,E_F)}{dE_F} g_{\mathrm{QD}}(E) dE, \tag{1}$$

where $f(E,E_F)$ is the Fermi-distribution with E_F denoting the Fermi-level position at the QD plane and E being the energy parameter for integration along the normalized distribution $g_{\mathrm{QD}}(E)$. e_n is the thermal emission rate of electrons from a given energy level to the conduction band. The factor $\Delta n_T(\omega, e_n)$ in Eq. (1) is the charge carrier exchange of the energy level distribution as a result of the Fermi-level oscillation in pace with the angular frequency, ω, of the probe signal from the capacitance meter

$$\Delta n_T(\omega, e_n) = \frac{e_n}{2\sqrt{4e_n^2 + \omega^2}} N_T, \tag{2}$$

where N_T is the concentration of QD energy states on a level determined by the Fermi-level. The dominating temperature dependence of e_n originates from a Boltzmann factor[9] $\exp[-\Delta E_n/(kT)]$, where ΔE_n is the energy level position below the conduction band edge and k is Boltzmann's constant. Lowering the temperature, therefore, quickly decreases, e_n, and thus the capacitance contribution from a specific energy level. This is the origin of the moving ledge in Fig. 2.

The total capacitance of the sample is expressed by

$$C = C_{\mathrm{cap}}(C_{\mathrm{QD}} + C_{\mathrm{buffer}})/(C_{\mathrm{cap}} + C_{\mathrm{QD}} + C_{\mathrm{buffer}}). \tag{3}$$

In an earlier published paper,[12] we used this treatment to explain the frequency dependence of the capacitance for samples similar to those used in the present work. By using similar data for the QD properties and the statistics used in Refs. 9 and 10, we find a theoretical plot of $-dC/dV = f(V,T)$, shown as a contour plot in Fig. 3. Two characteristic peaks, at (1 V, 60 K) and (1.6 V, 120 K), dominate the appearance of this graph. These two maxima occur when $-dC/dV$ has a resonance for the angular frequency $\omega = 2\pi \times 1$ MHz used in the calculation. Going back to the statistical theory,[9,14] we find that these peaks originate from a resonance with the maxima in s and p energy distributions, respectively.

Figure 4 shows experimental data corresponding to the theoretical plot of Fig. 3. Here, we observe three peaks: A at (1.8 V, 140 K), B at (0.9 V, 70 K), and C at (0.8 V, 60 K). Comparing with the theoretical plot, it is reasonable to identify A as originating from the s orbitals while B and C result from resonances with two of the p orbitals.[4] In earlier studies, we have demonstrated that DLTS data from QDs, with the same size distribution as those of the present samples, can be interpreted by considering the exchange interaction energies of the two possible s electrons as very small.[14] This

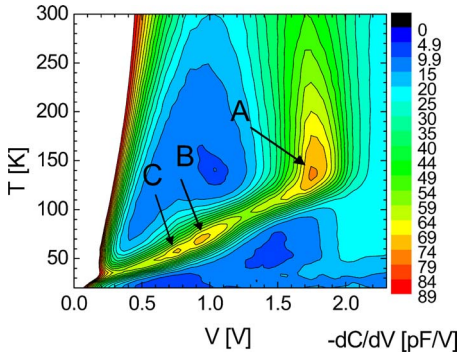

FIG. 4. (Color online) Experimental $-dC/dV$ spectra in a contour representation on the (V,T)-plane. Peaks A–C, indicated by arrows, are clearly resolved for contributions from electrons in the *s* shells (A) and in the *p* shells (B and C), respectively.

is confirmed in Fig. 4 by the single peak at a point where the *s* level contribution, according to the theoretical plot in Fig. 3, would be expected. Peaks B and C on the other hand exist in a (V,T) range where *p* electrons are anticipated in Fig. 3. In this calculation, only one *p* electron was considered. The two peaks in the experimental data of Fig. 4, therefore can be identified as originating from the first and the second *p* electron. This suggests that the exchange interaction energies for these orbitals are larger than for those of the *s* shell.

Using the $-dC/dV$ data to amplify the influence of QD excited states was done in an earlier work by Brunkov *et al.*[15] without scanning in temperature to find the extreme points in contour plots on the (V,T) plane. Such procedure was performed by measuring conductance as a function of temperature and reverse voltage by Chang *et al.*[16] thus revealing extreme points representing s and p levels. However, similar to corresponding data measured on MOS structures the measured conductance needs to be corrected for influence from capacitances involved in the equivalent circuit representing the device under test.[17]

In the present method, peaks, as shown in Fig. 4, occur on a voltage versus temperature plane as a result of the energy distribution of electrons and their dynamic interaction with the conduction band of the host crystal. Along the voltage coordinate, a peak is established when the Fermi-level in the neutral part of the buffer layer passes the maximum point of the confined electron state distribution. In the temperature direction, extreme points originate from the resonance between the thermal emission rate and the small-signal frequency used in the capacitance measurement. This gives rise to extreme points on the surface spanned by $-dC/dV = f(V,T)$ revealing the existence of electron eigenenergy states in the QDs, which are not easily obtained from 2D *C-V* data as shown in Fig. 2.

The authors are indebted to Dr. Mahdad Sadeghi of the MC2 Nanotechnology Facility for performing the MBE work. The work was financed by the European NANOSIL Network of Excellence (Grant No. IST-216171), the Chalmers MC2SOI project, and by the Polish Ministry of Science and Higher Education (Grant Nos. 3T11B00729 and 1.12.053)

[1]K. H. Schmidt, G. Medeiros-Ribeiro, M. Oestreich, P. M. Petroff, and G. H. Döhler, Phys. Rev. B **54**, 11346 (1996).
[2]S. Malik, E. C. LeRu, D. Childs, and R. Murray, Phys. Rev. B **63**, 155313 (2001).
[3]R. Heitz, M. Veit, N. N. Ledentsov, A. Hoffmann, D. Bimberg, V. M. Ustinov, P. S. Kop'ev, and Zh. I. Alferov, Phys. Rev. B **56**, 10435 (1997).
[4]B. T. Miller, W. Hansen, S. Manus, R. J. Luyken, A. Lorke, J. P. Kotthaus, S. Huant, G. Medeiros-Rebeiro, and P. M. Petroff, Phys. Rev. B **56**, 6764 (1997).
[5]S. D. Lin, V. V. Ilchenko, V. V. Marin, N. V. Shkil, A. A. Buyanin, K. Y. Panarin, and O. V. Tretyak, Appl. Phys. Lett. **90**, 263114 (2007).
[6]C. M. A. Kapteyn, F. Heinrichsdorff, O. Stier, R. Heitz, M. Grundmann, N. D. Zacharov, D. Bimberg, and P. Werner, Phys. Rev. B **60**, 14265 (1999).
[7]O. Engström, M. Malmkvist, Y. Fu, H. O. Olafsson, and E. Ö. Sveinbjörnsson, Appl. Phys. Lett. **83**, 3578 (2003).
[8]S. Schulz, S. Schnüll, Ch. Heyn, and W. Hansen, Phys. Rev. B **69**, 195317 (2004).
[9]O. Engström and P. T. Landsberg, Phys. Rev. B **72**, 075360 (2005).
[10]O. Engström, M. Kaniewska, W. Jung, and M. Karczmarczyk, Appl. Phys. Lett. **91**, 033110 (2007).
[11]O. Engström and M. Kaniewska, Nanoscale Res. Lett. **3**, 179 (2008).
[12]O. Engström, A. Eghtedari, and M. Kaniewska, Mater. Sci. Eng., C **27**, 936 (2007).
[13]O. Engström, B. Raeissi, and J. Piscator, J. Appl. Phys. **103**, 104101 (2008).
[14]O. Engström, P. T. Landsberg, and Y. Fu, Mater. Sci. Eng., C **26**, 739 (2006).
[15]P. N. Brunkov, A. R. Kovsh, V. M. Ustinov, Yu. G. Musikhin, N. N. Ledentsov, S. G. Konnikov, A. Polimeni, A. Patane, P. C. Main, L. Eaves, and C. M. A. Kapteyn, J. Electron. Mater. **28**, 486 (1999).
[16]W.-H. Chang, W. Y. Chen, M. C. Cheng, C. Y. Lai, T. M. Hsu, N.-T. Yeh, and J.-I. Chyi, Phys. Rev. B **64**, 125315 (2001).
[17]J. Piscator, B. Raeissi, and O. Engström, Appl. Phys. Lett. **94**, 213507 (2009).